Alfonso Fuentes

Faydor L. Litvin

Gear Research Center,
Department of Mechanical Engineering,
University of Illinois at Chicago,
Chicago, IL 60607-7022

Baxter R. Mullins

Ron Woods

Bell Helicopter Textron Inc.,
Forth Worth, TX 76101

Robert F. Handschuh

U.S. Army Research Laboratory,
NASA Glenn Research Center,
Cleveland, OH 44135

Design and Stress Analysis of Low-Noise Adjusted Bearing Contact Spiral Bevel Gears

An integrated computerized approach for design and stress analysis of low-noise spiral bevel gear drives with adjusted bearing contact has been developed. The computational procedure is an iterative process requiring four separate steps that provide: (a) a parabolic function of transmission errors that is able to reduce the effect of errors of alignment, and (b) reduction of the shift of bearing contact caused by misalignment. Application of finite element analysis permits the contact and bending stresses to be determined and the formation of the bearing contact to be investigated. The design of finite element models and boundary conditions is automated and does not require intermediate CAD computer programs. A commercially available finite element analysis computer program with contact capability is used to conduct the stress analysis. The theory developed is illustrated with numerical examples. [DOI: 10.1115/1.1481364]

1 Introduction

Spiral bevel gears have found broad application in helicopter and truck transmissions. Design and stress analysis of such gear drives is a recent topic of research that has been performed by many scientists [1–10]. Reduction of noise and stabilization of bearing contact of misaligned spiral bevel gear drives is still a very challenging topic of research although machine tool manufacturers have developed analysis tools and outstanding equipment for manufacture of such gear drives. The phenomenon of design of spiral bevel gears is that the machine-tool settings of spiral bevel gears are not standardized and have to be specially determined for each set of parameters of design to guarantee the required quality of the gear drives.

A new approach is proposed for the solution of this problem that is based on the following considerations:

(1) The gear machine-tool settings are considered as given (adapted, for instance, from the Gleason summary). The to-be-determined pinion machine-tool settings have to provide the observation of assigned conditions of meshing and contact of the gear drive.

(2) Low noise of the gear drive is achieved by application of a predesigned parabolic function of transmission errors of a limited value of maximum transmission error of 6–8 arcsec. A predesigned parabolic function of transmission errors is able to absorb almost linear discontinuous functions of transmission errors caused by errors of alignment that are the source of high noise and vibration [4,11]. The authors' concept of reduction of noise has been confirmed by test of prototypes of existing design and proposed design accomplished at NASA Glenn Research Center. The test showed that the level of noise was reduced by 18 decibels of the whole amount of 90 decibels and the vibration was reduced by 50% at the spiral bevel gear meshing frequencies and its harmonics [4].

(3) The provided orientation of the bearing contact has to reduce its shift caused by the errors of alignment of the gear drive.

(4) The developed procedure of design is an iterative process based on simultaneous application of local synthesis and TCA (Tooth Contact Analysis). The local synthesis provides assigned conditions of meshing and contact at the mean contact point of tangency of pinion-gear tooth surfaces. The TCA computer program can simulate the conditions of meshing and contact for the entire meshing process.

Finite element method is used for stress analysis and the investigation of the bearing contact. A model of three contacting teeth complemented with the boundaries conditions is applied for finite element analysis (FEA). A general purpose finite element analysis computer program [12] has been used to conduct the stress analysis. The design of contact models is automated and does not require application of CAD computer programs.

Computer programs for synthesis, analysis, and automation of FEA are based on application of the same programming language. Graphic representation of results of computation is obtained by application of a commercially available graphical program.

2 Basic Ideas of Developed Approach

Local Synthesis. The mean contact point M is chosen on gear tooth surface Σ_2 (Fig. 1). Parameters $2a$, η_2, and m'_{12} are taken at M and represent the mayor axis of the instantaneous contact ellipse, the tangent to the contact path on gear tooth surface, and the derivative of the gear ratio function $m_{12}=\omega^{(1)}/\omega^{(2)}$ where $\omega^{(1)}$ and $\omega^{(2)}$ are the angular velocities of the pinion and gear rotations.

The program of local synthesis enables the pinion machine-tool settings to be determined considering as known the gear machine-tool settings and parameters a, η_2, and m'_{12} [11]. The program requires solution of ten equations for ten unknowns but six of the ten equations are represented in echelon form. The algorithm of local synthesis includes relations between principal curvatures and directions proposed in [11,13–15].

TCA (Tooth Contact Analysis). The computer program algorithm is based on conditions of continuous tangency of pinion-gear tooth surfaces and is illustrated in Fig. 2. The TCA program enables the function of transmission errors $\Delta\phi_2(\phi_1)$ to be determined and the bearing contact to be obtained for each iteration whereas the input variable parameters a, η_2, and m'_{12} of the respective iteration are applied.

The computational procedure is divided into four separately applied procedures performed as follows:

Contributed by the Mechanisms and Robotics Committee for publication in the JOURNAL OF MECHANICAL DESIGN. Manuscript received December 2000. Associate Editor: M. Raghavan.

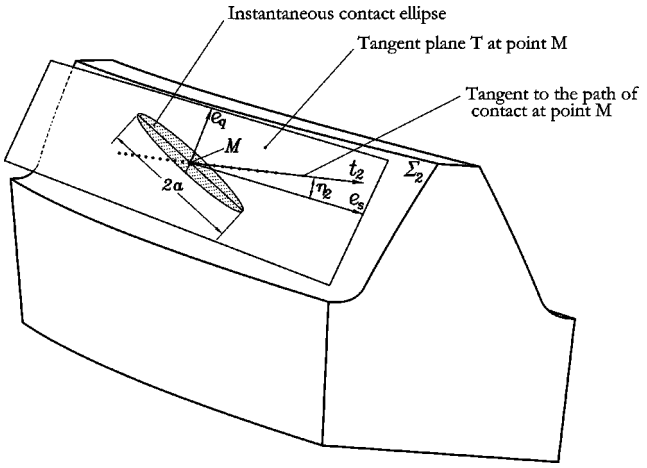

Fig. 1 Illustration of parameters η_2 and a applied for local synthesis

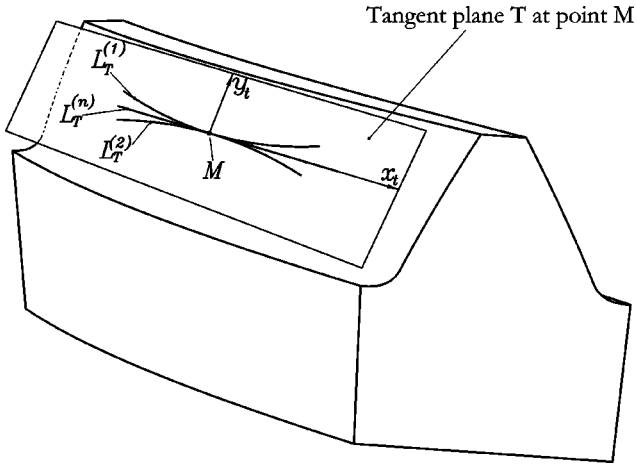

Fig. 3 Projections of various path of contact L_T on tangent plane T

Procedure 1: The purpose of the procedure is to obtain the assigned orientation of the bearing contact. The procedure is accomplished by the observation of the following conditions:

(a) The local synthesis and TCA are applied simultaneously whereas the variable parameter is m'_{12} and parameters a and η_2 are taken as constant. The orientation of η_2 is initially chosen as a longitudinally oriented bearing contact. The errors of alignment are taken equal to zero.

(b) Using the output of TCA it becomes possible to obtain numerically the path of contact on gear tooth surface Σ_2 and determine its projection L_T on plane T that is tangent to Σ_2 at M (Fig. 1).

(c) The goal of the iterative process (accomplished by simultaneous application of local synthesis and TCA) is to obtain $L_T^{(n)}$ as the straight line for the process of meshing of the cycle $-\pi/N_1 \leqslant \phi_1 \leqslant \pi/N_1$. This goal is achieved by variation of m'_{12} and the sought-for solution is obtained analytically as follows: (i)

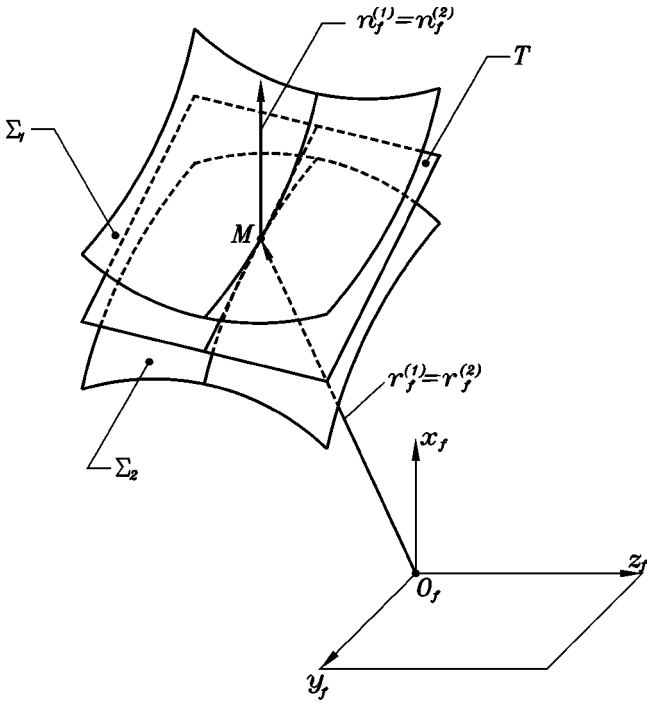

Fig. 2 Tangency of tooth surfaces of a gear drive

(i) The numerically obtained projection $L_T^{(i)}$ is represented by a polynomial function

$$y_t(x_t, m_{12}'^{(i)}) = \beta_0 (m'_{12})^{(i)} + \beta_1 (m'_{12})^{(i)} x_t + \beta_2 (m'_{12})^{(i)} x_t^2 \quad (1)$$

(ii) Variation of $m_{12}'^{(i)}$ $(i=1,2,3,\cdots,n)$ in the iterative process based on simultaneous application of local synthesis and TCA enables such a path of contact to be obtained when $\beta_2 = 0$ and $L_T^{(n)}$ becomes a straight line. Figure 3 shows various lines $L_T^{(1)}$, $L_T^{(2)}$, and the desired shape $L_T^{(n)}$ (Fig. 3).

(iii) The iterative process is directed at obtaining $\beta_2 (m'_{12})^{(i)}$ and is based on the secant method [16] that is illustrated with Fig. 4.

Procedure 2: Procedure 1 is accomplished obtaining $L_T^{(n)}$ as a straight line. However, the output of the TCA for the function of the transmission errors, function $\Delta\phi_2^{(n)}(\phi_1)$ where $-\pi/N_1 \leqslant \phi_1 \leqslant \pi/N_1$, is of unfavorable shape and magnitude. The goal is to transform $\Delta\phi_2^{(n)}(\phi_1)$ into a parabolic function and limit the magnitude of maximum transmission errors. This goal is achieved by application of *modified roll* for pinion generation.

Modified roll means that during the pinion generation the angles of rotation of the pinion and the cradle of the generating machine, ψ_1 and ψ_{c1}, respectively, are related as follows

$$\psi_1^{(j)}(\psi_{c1}) = m_{1c}\psi_{c1} - b_2\psi_{c1}^2 - b_3\psi_{c1}^3 \quad (2)$$

where m_{1c} is the first derivative of function $\psi_1(\psi_{c1})$ at $\psi_{c1}=0$ that is obtained by application of local synthesis [4]. The superscript j in Eq. (2) indicates that the j-th iteration is considered.

The purpose of procedure 2 is the transformation of the function of transmission errors $\Delta\phi_2^{(n)}(\phi_1)$ obtained at the final step of Procedure 1. This goal is achieved as follows:

(i) The local synthesis and TCA computer program are applied simultaneously and the errors of alignment of the gear drive are taken equal to zero.

(ii) The function of transmission errors $\Delta\phi_2^{(n)}(\phi_1)$ is the output of TCA obtained at the n-th iteration of Procedure 1 and is represented numerically. We represent $\Delta\phi_2^{(n)}(\phi_1)$ as a polynomial function of the third order designated as

$$\Delta\phi_2^{(j)}(\phi_1) = a_0^{(j)} + a_1^{(j)}\phi_1 + a_2^{(j)}\phi_1^2 + a_3^{(j)}\phi_1^3, \quad -\frac{\pi}{N_1} \leqslant \phi_1 \leqslant \frac{\pi}{N_1} \quad (3)$$

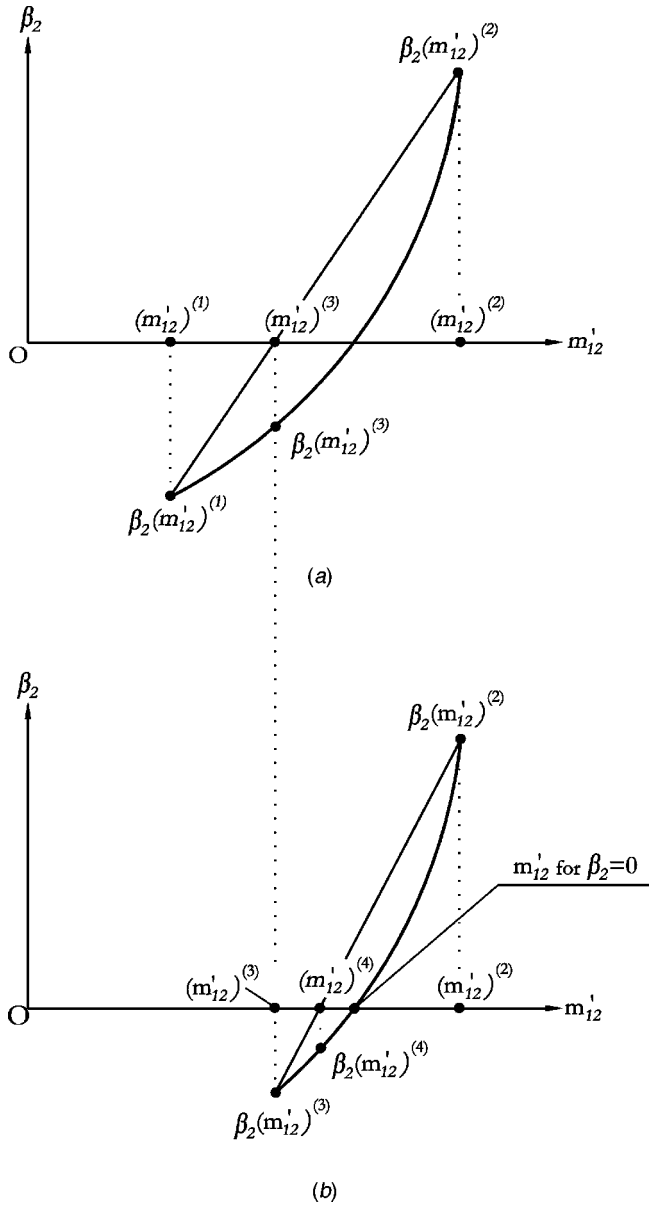

Fig. 4 Illustration of computations for determination of $\beta_2(m'_{12})$

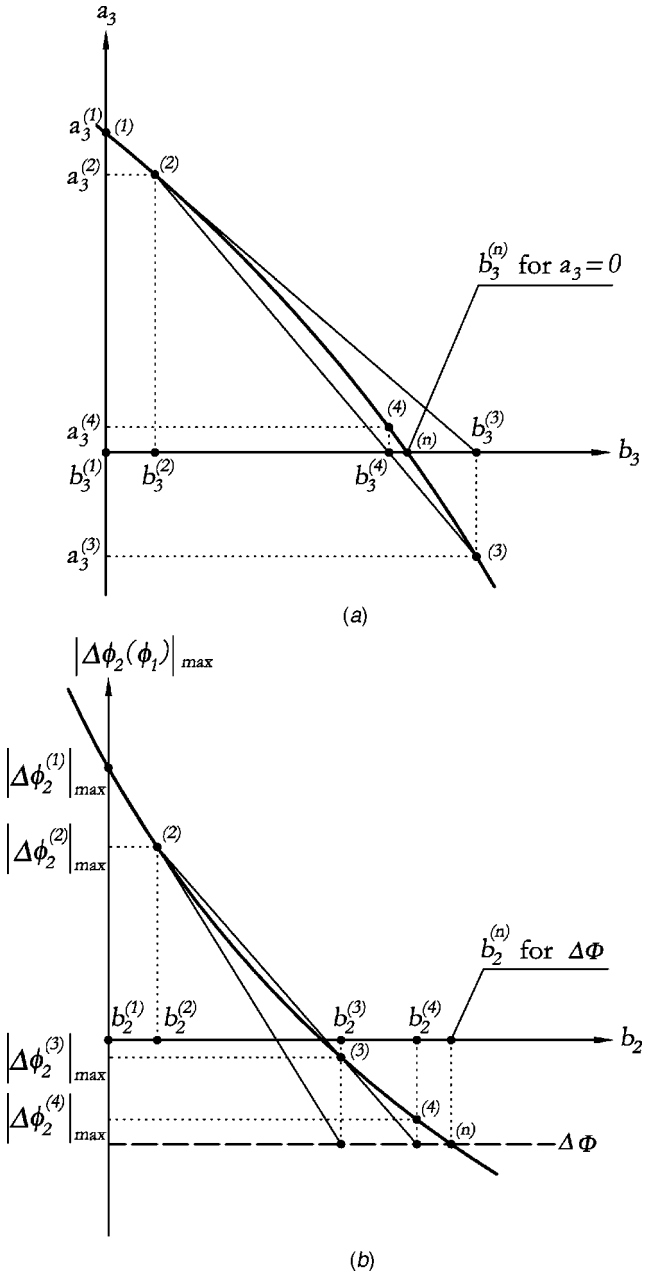

Fig. 5 Illustration of variation of coefficients b_2 and b_3 of modified roll

The designation $j=1,2,\cdots,k$ means that an iterative process for modification of $\Delta\phi_2^{(n)}(\phi_1)$ is considered. Function $\Delta\phi_2^{(1)}(\phi_1) \equiv \Delta\phi_2^{(n)}$ is obtained at the final iteration of Procedure 1.

(iii) The goal of Procedure 2 is to transform the function of transmission errors and obtain

$$\Delta\phi_2^{(k)}(\phi_1) = -a_2^{(k)}\phi_1^2, \quad -\frac{\pi}{N_1} \leqslant \phi_1 \leqslant \frac{\pi}{N_1} \tag{4}$$

$$|\Delta\phi_2^{(k)}(\phi_1)|_{\max} = a_2^{(k)}\left(\frac{\pi}{N_1}\right)^2 = \Delta\Phi \tag{5}$$

(iv) The goals mentioned above are obtained by variation of coefficients $b_2^{(j)}$ and $b_3^{(j)}$ of the function of modified roll. The secant method [16] is applied for this purpose whereas variations of $b_2^{(j)}$ and $b_3^{(j)}$ are performed separately and illustrated in Fig. 5.

Procedure 3: Procedures 1 and 2 discussed above enable to obtain: (i) a longitudinally oriented projection L_T of the path of contact and represent L_T is a straight line; (ii) a parabolic function of transmission errors with the assigned level of maximum transmission errors. However, these results have been obtained for an aligned gear drive.

The goal of Procedure 3 is to reduce the shift of the bearing contact caused by errors of alignment and this is achieved by the proper change of orientation of L_T assigned initially in Procedure 1. The procedure is based on the flow chart shown in Fig. 6.

Errors of alignment of the gear drive will cause the shift of the bearing contact but they will not affect the obtained function of transmission errors since it is a parabolic function that is able to absorb the linear functions of transmission errors caused by misalignment [11,13–15].

Procedure 3 is performed as follows:

(i) Computer programs developed for local synthesis and TCA are again applied simultaneously, but the expected errors of alignment are simulated.

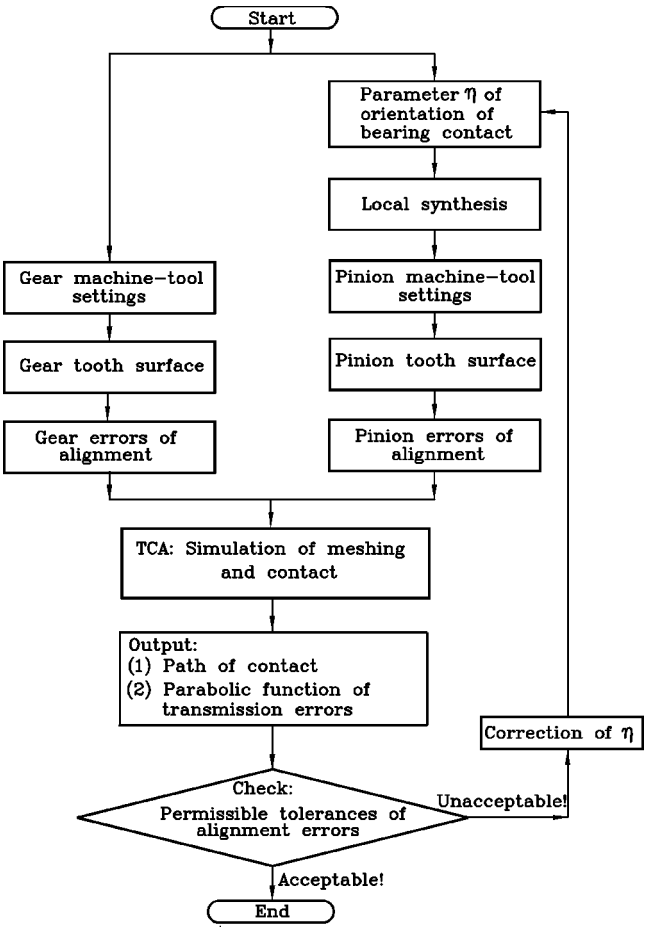

Fig. 6 Flow chart for procedure 3

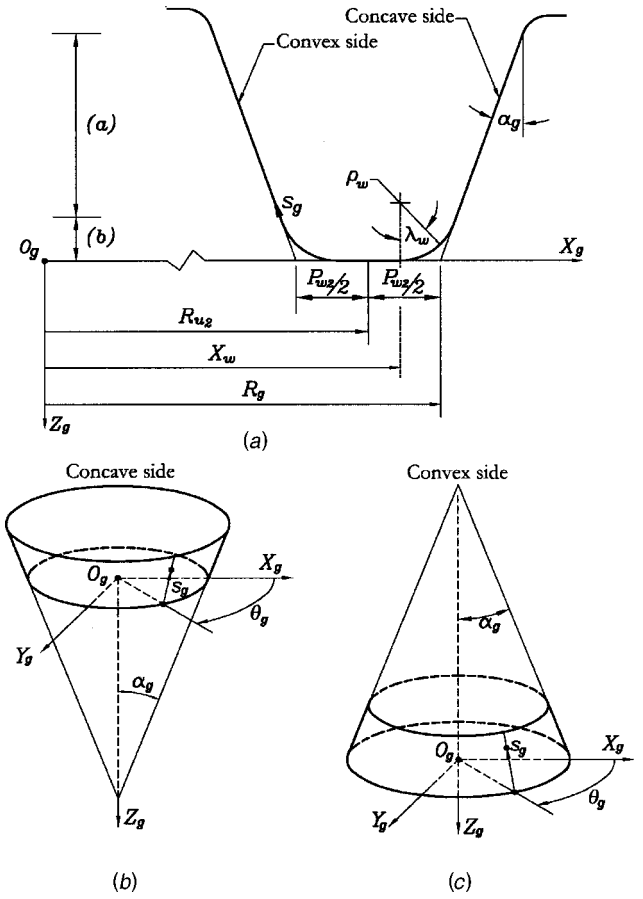

Fig. 7 Blade and generating cones for gear generating tool: (*a*) illustration of head-cutter blade; (*b*) *y* (*c*) generating tool cones for concave and convex sides

(ii) The effect of all errors of alignment on the shift of the bearing contact is investigated separately. The sensitivity of the shift of L_T is reduced by the proper choice of parameter η_2 (Fig. 1). Thus, the variable parameter of the local synthesis in Procedure 3 is η_2.

(iii) Application of procedure 3 causes that finally L_T will be chosen as the deviated from the longitudinally one. The deviation depends on the design parameters of the gear drive, particularly on the gear ratio m_{12} (see Section 6), and on the errors of alignment that are applied.

Procedure 4: After completion of Procedures 1, 2, and 3, the obtained pinion machine-tool settings guarantee that the designed gear drive is indeed a low-noise gear drive with reduced sensitivity to errors of alignment (see numerical examples of design in Section 6).

The goal of Procedure 4 is the stress analysis and the investigation of formation of the bearing contact whereas the contact ratio is $m_c>1$ (see Section 5). The approach developed for finite element analysis (FEA) has the following advantages:

1 The computer language applied for automation of FEA is the same as applied for the synthesis and analysis of the gear drive.

2 The contacting model (formed by three teeth of the pinion and the gear and the boundary conditions) is determined automatically. There is no need in application of intermediate CAD computer programs to develop the finite element models for application of FEA (see details in Section 5).

3 Derivation of Equations of Gear Tooth Surfaces

Remember at this point that the machine-tool settings for the gear are considered as given and the to-be-derived equations allow the gear tooth surfaces to be determined. The head-cutter is provided with blades that are rotated about the Z_g-axis of the head-cutter (Fig. 7) during the process of generation. Both sides of the gear tooth are generated simultaneously. The profile of the blade consists of two parts (Fig. 7): (i) of a straight line, and (ii) of a fillet formed by two circular arcs connected by a straight line. The blades by rotation about the Z_g-axis form the head-cutter generating surfaces.

Applied Coordinate Systems. Coordinate system S_{m_2}, S_{a_2}, S_{b_2} are the fixed ones and they are rigidly connected to the cutting machine (Fig. 8). The movable coordinate systems are S_2 and S_{c_2} rigidly connected to the gear and the cradle, respectively. Coordinate system S_g is rigidly connected to the gear head-cutter. It is considered that the head-cutter is a cone, and the rotation of the head cutter about the Z_g-axis does not affect the process of generation. The head-cutter is mounted on the cradle and coordinate system S_g is rigidly connected to the cradle coordinate system S_{c_2}. The cradle and the gear perform related rotations about the Z_{m_2}-axis and the Z_{b_2}-axis, respectively. Angles ψ_{c2} and ψ_2 are related and represent the current angles of rotation of the cradle and the gear. The ratio of gear roll is designated as m_{2c_2} and is determined as

$$m_{2c_2}=\frac{\omega^{(2)}}{\omega^{(c_2)}}=\frac{d\psi_2}{dt}\div\frac{d\psi_{c2}}{dt} \tag{6}$$

The installment of the tool on the cradle is determined by parameters S_{r_2} and q_2, that are called radial distance and basic

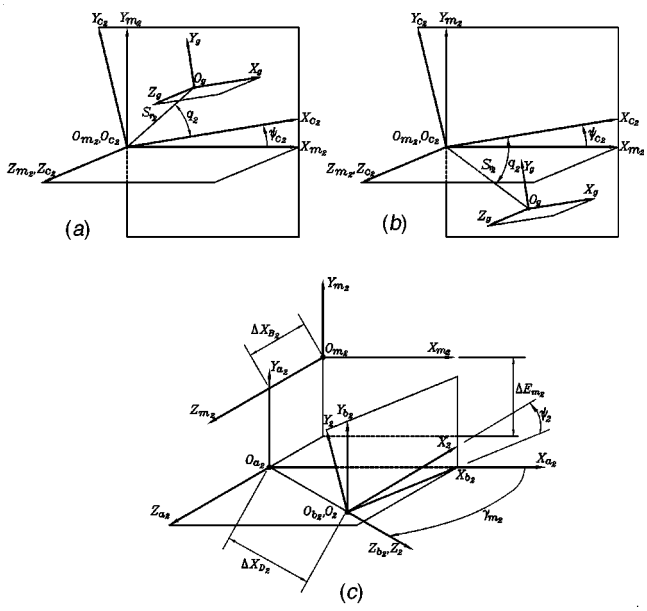

Fig. 8 Coordinate systems applied for gear generation: (*a*) and (*b*) illustration of tool installment for generation of right- and left-hand gears; (*c*) illustration of corrections of machine-tool settings

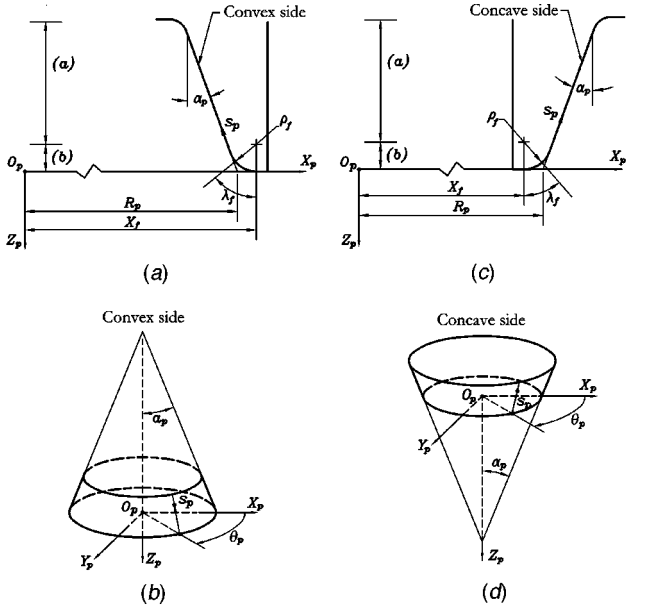

Fig. 9 Blades and generating cones for pinion generating tool: (*a*) convex side blade; (*b*) convex side generating cone; (*c*) concave side blade; (*d*) concave side generating cone

cradle angle. Parameters ΔX_{B_2}, ΔE_{m_2}, ΔX_{D_2}, and γ_{m_2} represent the settings of the gear. Figs. 8(*a*) and 8(*b*) show the installment of the head-cutter for right hand and left hand gears respectively.

Procedure of Derivation. The head-cutter generating surface is represented in coordinate system S_g by the vector function $r_g(S_g, \theta_g)$ where s_g and θ_g are the surface parameters.

The family of generating surfaces is represented in coordinate system S_2 rigidly connected to the gear by the matrix equation

$$\mathbf{r}_2(s_g, \theta_g, \psi_2) = \mathbf{M}_{2g}(\psi_2)\mathbf{r}_g(s_g, \theta_g) \tag{7}$$

where ψ_2 is the generalized parameter of motion.

The equation of meshing is determined as

$$f_{2g}(s_g, \theta_g, \psi_2) = 0 \tag{8}$$

determined as [11,14]

$$\left(\frac{\partial \mathbf{r}_2}{\partial \theta_g} \times \frac{\partial \mathbf{r}_2}{\partial s_g}\right) \cdot \frac{\partial \mathbf{r}_2}{\partial \psi_2} = 0 \tag{9}$$

or as [11,13,14]

$$\mathbf{N}_g \cdot \boldsymbol{\nu}_g^{(g2)} = 0 \tag{10}$$

Here $\mathbf{N}_g(s_g, \theta_g)$ is the normal to the head-cutter surface represented in coordinate system S_g and $\boldsymbol{\nu}_g^{(g2)}$ is the relative velocity represented in S_g.

Equations (7) and (8) determine the gear tooth surface by three related parameters.

4 Derivation of Pinion Tooth Surfaces

The two sides of the pinion tooth surfaces are generated separately. The machine-tool settings applied for generation of each tooth side are determined separately by application of Procedures 1, 2, and 3 mentioned above. Profile blades of pinion head-cutters are represented in Fig. 9.

Applied Coordinate Systems. Coordinate systems applied for generation of pinion are shown in Fig. 10. Coordinate systems S_{m_1}, S_{a_1}, S_{b_1} are the fixed ones and they are rigidly connected to the cutting machine. The movable coordinate systems S_1 and S_{c_1} are rigidly connected to the pinion and the cradle, respectively. Systems S_1 and S_2 are rotated about the Z_{m_1}-axis and Z_{b_1}-axis, respectively, and their rotations are related by a polynomial function $\psi_1(\psi_{c1})$ wherein modified roll is applied (see below). The ratio of instantaneous angular velocities of the pinion and the cradle is defined as $m_{1c}(\psi_1(\psi_{c1})) = \omega^{(1)}(\psi_{c1})/\omega^{(c)}$. The magnitude $m_{1c}(\psi_1)$ at ψ_{c1} is called ratio of roll or velocity ratio. Parameters ΔX_{D_1}, ΔX_{B_1}, ΔE_{m_1}, γ_{m_1} are the basic machine tool settings for pinion generation.

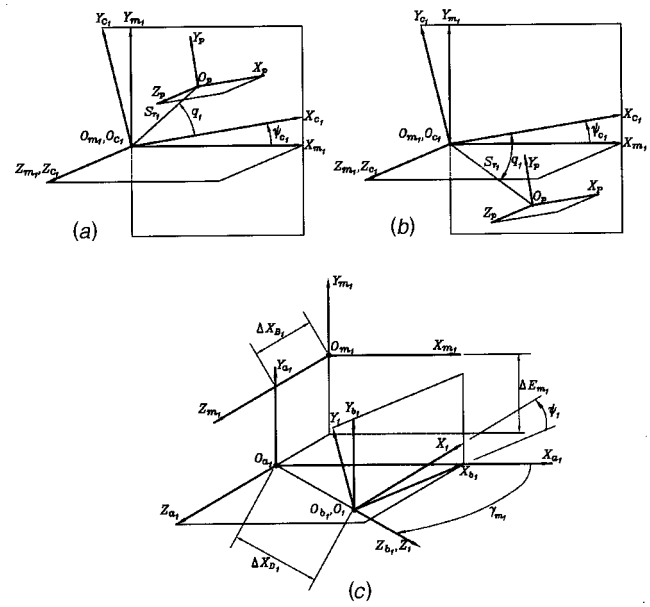

Fig. 10 Coordinate systems applied for the pinion generation: (*a*) and (*b*) illustration of tool installment for generation of right- and left-hand gears; (*c*) illustration of corrections of machine-tool settings

Procedure of Derivation. The pinion head-cutter surface is represented by vector function $\mathbf{r}_p(s_p,\theta_p)$ (Fig. 9) where (s_p,θ_p) are the surface parameters.

The family of head-cutters is represented in coordinate system S_1 rigidly connected to the pinion by the matrix equation

$$\mathbf{r}_1(s_p,\theta_p,\psi_{c1})=\mathbf{M}_{1p}(\psi_{c1})\mathbf{r}_p(s_p,\theta_p) \tag{11}$$

Unlike the case of gear generation, modified roll is applied for the generation of the pinion, and function $\psi_1(\psi_{c1})$ relates the angles of rotation of the pinion and the cradle of the pinion generating machine by a polynomial but not linear function (see Eq. (2)).

The equation of meshing is determined as

$$f_{p1}(s_p,\theta_p,\psi_{c1})=0 \tag{12}$$

that is derived by application of two following alternative approaches [11,13,14]:

$$\left(\frac{\partial\mathbf{r}_1}{\partial\theta_p}\times\frac{\partial\mathbf{r}_1}{\partial s_p}\right)\cdot\frac{\partial\mathbf{r}_1}{\partial\psi_{c1}}=0 \tag{13}$$

or

$$\mathbf{N}_p\cdot\boldsymbol{\nu}_p^{(p1)}=0 \tag{14}$$

where $\mathbf{N}_p$ is the normal to pinion head-cutter surface Σ_p that is represented in S_p.

Equations (11) and (12) represent the pinion tooth surfaces by three related parameters.

5 Application of Finite Element Analysis

Application of finite element analysis permits the following:

(1) Investigation of the bearing contact when multiple sets of teeth may be in contact under load simultaneously.
(2) Determination of contact and bending stresses.

Application of finite element method [17] requires the development of the finite element mesh, definition of possible contacting surfaces, and the establishment of boundary conditions to load the gear drive with the desired torque. Finite element analysis is performed by application of general purpose computer program [12].

The authors have developed a modified approach to perform the finite element analysis that has the following advantages:

(a) The same programming language is applied for synthesis, analysis, and generation of finite element models of the gear drives. Graphic interpretation of the output is obtained by using commercially available graphical program.

(b) The generation of the finite element mesh required for finite element analysis is performed automatically using the equations of the surfaces of the tooth and its portion of the rim. Nodes of the finite element mesh lying on the tooth surfaces of pinion (gear) are guaranteed to be points of the real tooth surfaces of the pinion (gear). Loss of accuracy due to the development of solid models using CAD computer programs is avoided. The boundary conditions for the pinion and the gear are set automatically as well.

(c) Investigation of the bearing contact for a cycle of meshing permits investigation of the influence of the contact ratio m_c (whereas the contact is formed on neighboring tooth surfaces if $m_c>1$) and find out the possibility of edge contact.

(d) There is no need to apply CAD computer programs for development of finite element models.

The development of the solid models and finite element meshes using CAD computer programs is time expensive, requires skilled users of used computer programs, and has to be done for every case of gear geometry and position of meshing to be investigated.

The developed approach is free of all these disadvantages and is summarized as follows:

Step 1: Using the equations of both sides of tooth surfaces and the portions of the corresponding rim, we may represent analytically the volume of the designed body. Fig. 11(*a*) shows the designed body for one-tooth model of the pinion of a spiral bevel gear drive.

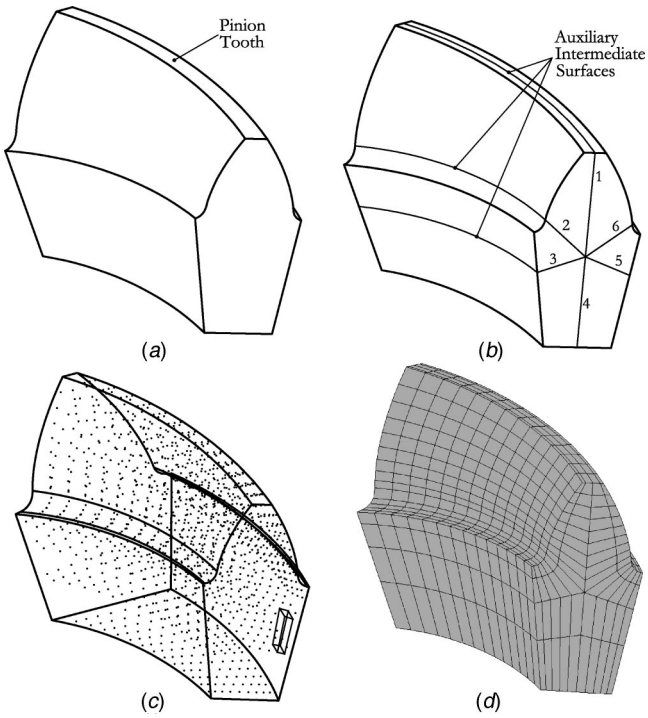

Fig. 11 Illustrations of (*a*) the volume of designed body, (*b*) auxiliary intermediate surfaces, (*c*) determination of nodes for the whole volume, and (*d*) discretization of the volume by finite elements

Step 2: Auxiliary intermediate surfaces 1 to 6 shown in Fig. 11(*b*) may be determined. Surfaces 1 to 6 enable to divide the tooth in six subvolumes and control the discretization of these tooth subvolumes into finite elements.

Step 3: Analytical determination of node coordinates is performed taking into account the number of desired elements in longitudinal and profile direction (Fig. 11(*c*)). We emphasize that all nodes of the finite element mesh are determined analytically and those lying on the tooth surfaces are indeed points belonging to the real surfaces.

Step 4: Discretization of the model by finite elements using nodes determined in previous step is accomplished as shown in Fig. 11(*d*).

In the developed approach for finite element analysis, the torque is applied directly to the pinion and is transmitted to the gear through the contact between the pinion and the gear tooth surfaces. No assumption of normal tooth load or load distribution over the surfaces is required. The contact area is obtained as the result of finite element analysis.

6 Numerical Examples

Three examples of design of face-milled spiral bevel gears with different design parameters have been accomplished for the illustration of the developed theory. Details of the examples of design are represented in Appendix 1. A torque of 700 N·m has been applied to the pinion of examples 1 and 2. A torque of 300 N·m has been applied to the pinion of example 3. The material is steel with the properties of Young's Modulus $E=2.068\times10^8$ mN/mm^2 and Poisson's ratio 0.29. The output from the computations for the examples given are represented in Fig. 12 that shows:

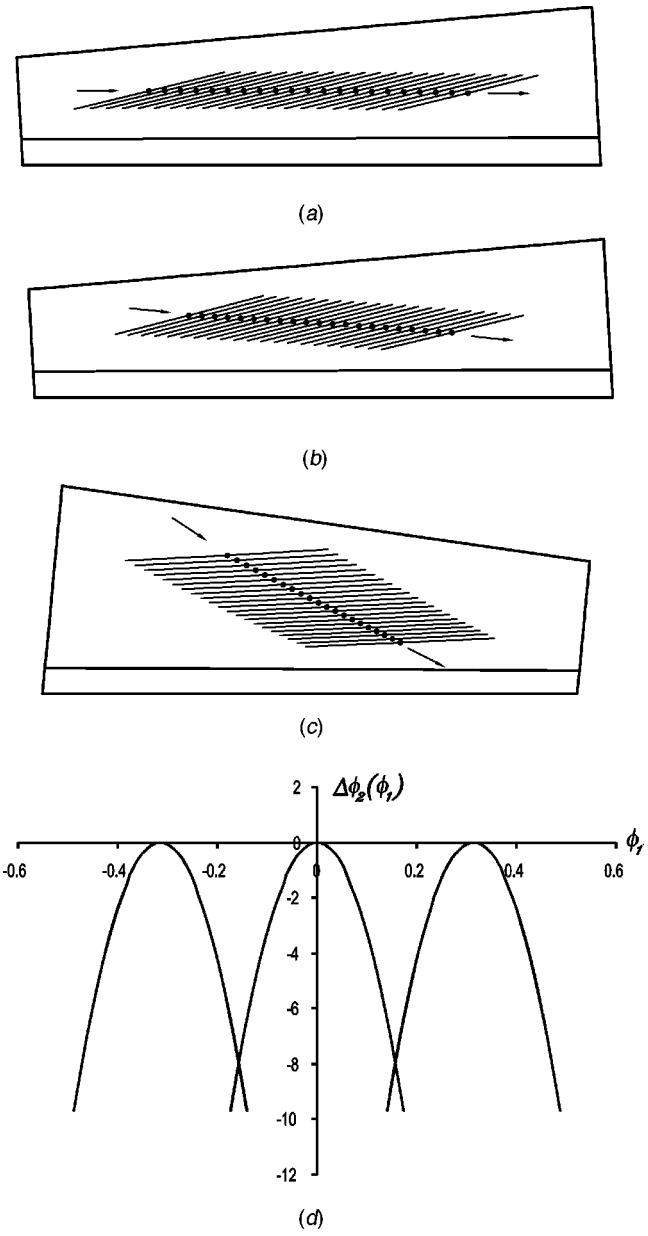

Fig. 12 Bearing contact and predesigned function of transmission errors: (*a*) longitudinally oriented bearing contact for gear drive of example 1; (*b*) adjusted bearing contact for gear drive of example 2; (*c*) adjusted bearing contact for gear drive of example 3; (*d*) function of transmission errors for examples 1, 2, and 3

(i) The bearing contact has a longitudinal direction in example 1 for an aligned gear drive (Fig. 12(*a*)).

(ii) The bearing contact in example 2 (Fig. 12(*b*)) is deviated from the longitudinal direction to reduce the shift of bearing contact caused by errors of alignment.

(iii) Example 3 of design (Fig. 12(*c*)) shows that the gear drive with a gear ratio close to 1 ($N_2/N_1=26/17$) is very sensitive to errors of alignment. The shift of bearing contact due to misalignment is reduced by larger deviation of the bearing contact from the longitudinal direction.

(iv) The function of transmission errors (Fig. 12(*d*)) for all three examples is indeed a parabolic function up to 8 arcsec of maximum amount.

Finite element analysis has been performed for all three examples. First order elements have been used to form the finite element mesh. Such elements are enhanced by incompatible nodes to improve their bending behavior. The total number of elements is 33606 with 42076 nodes for each finite element model. Figure 13 shows the 3-pair-of-teeth finite element mesh for example 2.

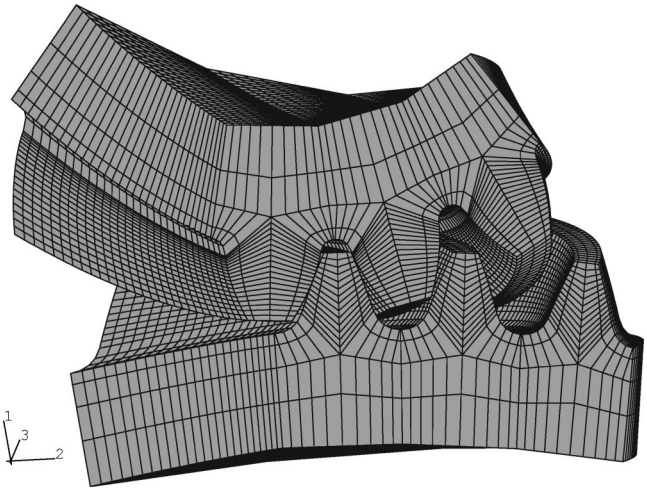

Fig. 13 Three-pair-of-teeth finite element mesh for example 2

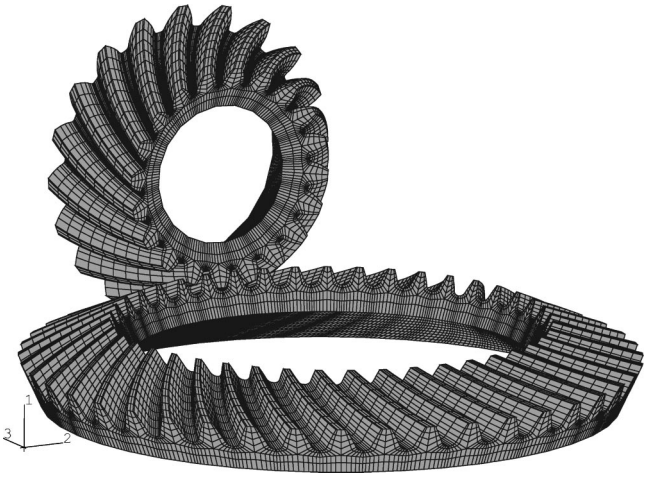

Fig. 14 Whole gear drive finite element mesh for example 2

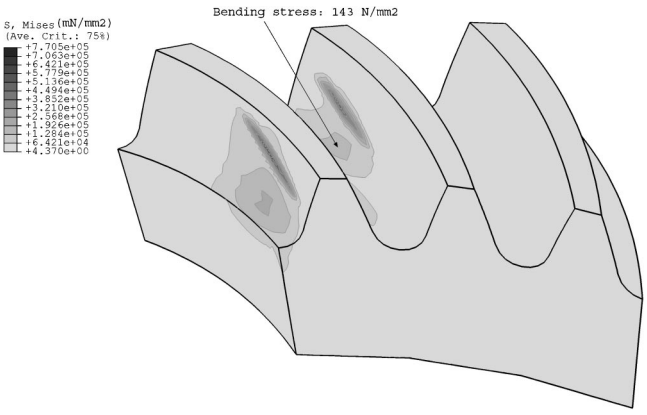

Fig. 15 Formation of the bearing contact in example 2 at the heel position of the gear

Figure 14 shows the whole gear drive finite element mesh.

The accomplished stress analysis has enabled the contact and bending stresses to be obtained. Von Mises equivalent stress is used to represent the stress distribution. The units used are mN/mm^2. Figure 15 shows the formation of the bearing contact in example 2 at the heel position of the gear. The maximum fillet stress at this position of contact is 143 N/mm^2 when a torque of 700 N·m is applied to the pinion (Fig. 15).

7 Conclusions

Based on the study conducted the following conclusions can be made:

(1) An integrated computerized approach has been developed for design of low-noise spiral bevel gears with an adjusted bearing contact based on the following ideas:

(i) Application of a parabolic function of transmission errors with limited values of maximum transmission errors permits to absorb linear discontinuous functions of transmission errors caused by misalignment and limit transmission errors.

(ii) The orientation of the bearing contact is adjusted to reduce the shift of contact caused by errors of alignment.

(iii) The approach developed is an iterative procedure based on simultaneous application of local synthesis and TCA (Tooth Contact Analysis) using modified roll for pinion generation.

(iv) The contacting model for finite element analysis is formed by three teeth and the boundary conditions, it is automatically designed and does not need intermediate CAD computer programs for application of finite element analysis.

(v) The same computer language is used for numerical computations performed for all stages of design, and automatic generation of finite element models. The developed theory is illustrated with three numerical examples.

(2) The approach developed may also be applied for design of formate cut spiral bevel gears, hypoid gear drives and other gear drives.

Acknowledgments

The authors express their deep gratitude to the Army Research Office, NASA Glenn Research Center, the Bell Helicopter Co. and the Gleason Foundation for the support of this research project.

Nomenclature

$\alpha_k (k=g,p)$ = blade angle of gear ($k=g$) and pinion ($k=p$) head-cutters (Figs. 7, 9)

$\beta_i (i=0,1,2)$ = coefficients of numerically obtained polynomial function for presentation of projection of path of contact on tangent plane T

$\gamma_{m_i} (i=1,2)$ = angles of pinion ($i=1$) and gear ($i=2$) root cones, respectively (Figs. 8, 10)

$\eta_i (=1,2)$ = parameter for presentation of tangent to the path of contact on the pinion ($i=1$) and gear ($i=2$) tooth surfaces respectively (Fig. 1)

θ_p, θ_g = surface parameters of the pinion and gear head cutters, respectively (Figs. 7, 9)

λ_f, λ_w = surface parameters of the pinion and gear fillet parts of the head cutter (Figs. 7, 9)

$\psi_{c_i} (i=1,2)$ = angle of rotation of the cradle in the process for generation of the pinion ($i=1$) or gear ($i=2$) (Figs. 8, 10)

$\psi_i (i=1,2)$ = angle of rotation of the pinion ($i=1$) or gear ($i=2$) in the process for generation (Figs. 8, 10)

ρ_f, ρ_w = fillet radii for the pinion and the gear (Figs. 7, 9)

$\omega^{(i)} (i=1,2)$ = angular velocity of the pinion ($i=1$) or gear ($i=2$) (in meshing and generation)

$\Sigma_i (i=1,2)$ = pinion ($i=1$) or gear ($i=2$) tooth surfaces

$\Sigma_k (k=p,g)$ = pinion ($k=p$) or gear ($k=g$) generating surfaces

$\Delta\phi_2(\phi_1)$ = function of transmission errors

$\Delta\Phi$ = maximal level of transmission errors (Fig. 5)

$\Delta A_1, \Delta A_2$ = pinion and gear axial displacements, respectively

$\Delta E, \Delta\gamma$ = offset and change of shaft angle due to errors of alignment, respectively

ΔE_{m_i} = blank offset of pinion ($i=1$) or gear ($i=2$) (Figs. 8, 10)

ΔX_{B_i} = sliding base for pinion ($i=1$) or gear ($i=2$) (Figs. 8, 10)

ΔX_{D_i} = machine center to back for pinion ($i=1$) or gear ($i=2$) (Figs. 8, 10)

$a_i (i=0,1,2,3)$ = coefficients of polynomial functions $\Delta\phi_2(\phi_1)$ of transmission errors

L_T = projection of path of contact on the tangent plane T (Fig. 3)

m'_{12} = second derivative of transmission function $\phi_2(\phi_1)$

m_{12} = gear ratio

m_{1c} = ratio of pinion roll

m_{2c_2} = ratio of gear roll

M = mean contact point (Figs. 1, 3)

$\mathbf{M}_{ji}, \mathbf{L}_{ji}$ = matrices of coordinate transformation from system S_i to system S_j

$\mathbf{n}_i^{(k)}, \mathbf{N}_i^{(k)}$ = unit normal and normal to surface Σ_k represented in coordinate system S_i

$q_i (i=1,2)$ = installment angle for head-cutter of the pinion ($i=1$) and gear ($i=2$) (Figs. 8, 10)

R_p, R_g = head-cutter point radius for the pinion and gear (Figs. 7, 9)

$\mathbf{r}_i$ = position vector represented in system S_i ($i=1,2,b_1,b_2,h,l,m_1,m_2,p,g$)

s_p, s_g = surface parameters of the pinion and gear (Figs. 8, 10)

S_i = coordinate system ($i=1,2,b_1,b_2,h,l,m_1,m_2,p,g$)

$S_{r_i} (i=1,2)$ = radial setting of the head-cutter of the pinion ($i=1$) and gear ($i=2$) (Figs. 8, 10)

$\boldsymbol{\nu}^{(ij)}$ = relative velocity at contact point ($i,j=1,2,c_1,c_2,p,g$)

Appendix

Table 1 Blank data

Appendix 1

	Examples 1, 2		Example 3	
	Pinion	Gear	Pinion	Gear
Number of teeth of the pinion and gear	20	43	17	26
Diametral pitch (1/mm)	0.1676		0.2600	
Shaft angle (deg.)	90.0000		90.0000	
Mean spiral angle (deg.)	32.0000	32.0000	30.0000	30.0000
Hand of spiral	RH	LH	LH	RH
Face width (mm)	41.0000	41.0000	20.3700	20.3700
Mean cone distance (mm)	120.9400	120.9400	49.5600	49.5600
Whole depth (mm)	11.2600	11.2600	8.4400	8.4400
Pitch angles (deg.)	24.9439	65.0561	33.1785	56.8215
Root angles (deg.)	23.1666	61.8166	30.4500	51.4000
Face angles (deg.)	28.1833	66.8333	38.6000	59.5500
Clearance (mm)	1.1200	1.1200	0.9100	0.9100
Addendum (mm)	6.8900	3.2500	5.0200	2.5100
Dedendum (mm)	4.3700	8.0100	3.4200	5.9300

Table 2 Parameters and installment settings of the gear head-cutter

	Examples 1, 2	Example 3
Average cutter diameter R_{u2} (mm) (Fig. 7)	152.4000	44.4500
Point width P_{w2} (mm) (Fig. 7)	3.5560	1.7780
Pressure angle, concave α_g (outside blade) (deg.) (Fig. 7)	20.0000	20.0000
Pressure angle, convex α_g (inside blade) (deg.) (Fig. 7)	20.0000	25.0000
Root fillet radius, concave and convex ρ_w (mm) (Fig. 7)	2.4130	1.1430
Machine center to back ΔX_{D_2} (mm) (Fig. 8)	0.0000	0.0000
Sliding base ΔX_{B_2} (mm) (Fig. 8)	0.0000	0.2000
Blank offset ΔE_{m_2} (mm) (Fig. 8)	0.0000	0.0000
Radial distance S_{r_2} (mm) (Fig. 8)	135.2870	53.5653
Machine root angle γ_{m_2} (deg.) (Fig. 8)	61.8166	51.4000
Cradle angle q_2 (deg.) (Fig. 8)	72.8081	54.3532
Velocity ratio m_{2c_2}	1.1011	1.2250

Table 3 Parameters and installment settings of the pinion head-cutter

	Example 1		Example 2		Example 3	
	Concave	Convex	Concave	Convex	Concave	Convex
Cutter point diameter R_p (mm) (Fig. 9)	152.7502	152.2802	152.6964	152.3493	40.4643	48.2959
Pressure angle α_p (deg.) (Fig. 9)	18.0000	22.0000	18.0000	22.0000	25.0000	20.0000
Root fillet radius ρ_f (mm) (Fig. 9)	1.0160	1.0160	1.0160	1.0160	0.7620	0.7620
Machine center to back ΔX_{D_1} (mm) (Fig. 10)	2.2268	-1.7319	2.2066	-1.8271	-1.2392	0.7604
Sliding base ΔX_{B_1} (mm) (Fig. 10)	-0.8572	0.7002	-0.8492	0.7376	0.0559	-0.9574
Blank offset ΔE_{m_1} (mm) (Fig. 10)	11.4197	-11.8235	7.7182	-6.8138	1.8219	-1.5402
Radial distance S_{r_1} (mm) (Fig. 10)	125.3700	145.6443	128.8831	140.9091	52.1695	55.2535
Machine root angle γ_{m1} (deg.) (Fig. 10)	23.1666	23.1666	23.1666	23.1666	30.4500	30.4500
Cradle angle q_1 (deg.) (Fig. 10)	73.0017	71.9026	73.4721	71.3245	-54.5158	-44.4546
Velocity ratio m_{1c}	2.2467	2.4848	2.2941	2.4260	1.8286	1.9251
Coefficient b_2 of modified roll (Eq. (2))	0.00011	-0.00012	0.00006	-0.00005	-0.00002	-0.00013
Coefficient b_3 of modified roll (Eq. (2))	0.02845	-0.03079	0.01772	-0.01579	0.00582	-0.00852

Table 4 Parameters for local synthesis

	Example 1		Example 2		Example 3	
	Concave	Convex	Concave	Convex	Concave	Convex
Direction of path of contact η_2 (deg.) (Fig. 1)	154.0000	171.0000	152.0000	168.0000	148.0000	155.0000
Length major axis contact ellipse $2a$ (mm) (Fig. 1)	12.0000	12.0000	12.0000	12.0000	8.0000	9.0000
Derivative of gear ratio function m'_{12}	0.003144	-0.003144	0.003144	-0.002555	-0.002555	0.002555
Elastic approach δ (mm)	0.00635	0.00635	0.00635	0.00635	0.00635	0.00635

Table 5 Errors of alignment allowed in examples 2 and 3

	Example 2		Example 1	
	Maximal	Minimal	Maximal	Minimal
Axial displacement of the pinion, ΔA_1	0.320 mm	-0.350 mm	0.100 mm	-0.060 mm
Axial displacement of the gear, ΔA_2	0.250 mm	-0.150 mm	0.200 mm	-0.150 mm
Change of shaft angle, $\Delta\gamma$	1.000 deg.	-0.800 deg.	1.000 deg.	-1.000 deg.
Shortest distance between axes, ΔE	0.150 mm	-0.100 mm	0.100 mm	-0.100 mm

References

[1] Handschuh, R. F., and Litvin, F. L., 1991, "A Method for Determining Spiral-Bevel Gear Tooth Geometry for Finite Element Analysis," *NASA Technical Paper 3096, AVSCOM Technical Report 91-C-020*.

[2] Lewicki, D. G., Handschuh, R. F., Henry, Z. S., and Litvin, F. L., 1994, "Low-Noise, High Strength Spiral Bevel Gears for Helicopter Transmission," J. Propul. Power, **10**(3) pp. 356–361.

[3] Litvin, F. L., Egelja, A., Tan, J., and Heath, G., 1998, "Computerized Design, Generation and Simulation of Meshing of Orthogonal Offset Face-Gear Drive with a Spur Involute Pinion with Localized Bearing Contact," Mech. Mach. Theory, **33**, pp. 87–102.

[4] Litvin, F. L., Wang, A. G., and Handschuh, R. F., 1996, "Computerized Generation and Simulation of Meshing and Contact of Spiral Bevel Gears with Improved Geometry," Comput. Methods Appl. Mech. Eng., **158**, pp. 33–64.

[5] Stadtfeld, H. J., 1993, *Handbook of Bevel and Hypoid Gears: Calculation, Manufacturing, and Optimization*, Rochester Institute of Technology, Rochester, New York.

[6] Stadtfeld, H. J., 1995, *Gleason Bevel Gear Technology-Manufacturing, Inspection and Optimization, Collected Publications*, The Gleason Works, Rochester, New York.

[7] Stadtfeld, H. J., and Gaiser, U., 2001, "The Ultimate Motion Graph," ASME J. Mech. Des., **122**(3), pp. 317–322.

[8] Bär, G., 2000, "Accurate Tooth Contact Determination and Optimization for Hypoid Bevel Gears using Automatic Differentiation," *4th World Congress on Gearing and Power Transmission*, pp. 519–529.

[9] Krenzer, T. J., 1981, *Tooth Contact Analysis of Spiral Bevel Gears and Hypoid Gears Under Load*, The Gleason Works, Rochester, New York.

[10] Gosselin, C., Cloutier, L., and Nguyen, Q. D., 1992, "The Influence of the Kinematical Motion Error on the Loaded Transmission Error of Spiral Bevel Gears," *AGMA paper 92FTM10*.

[11] Litvin, F. L., 1994, *Gear Geometry and Applied Theory*, Prentice Hall, Englewood Cliffs, New Jersey.

[12] Hibbit, Karlsson & Sorensen, Inc., 1998, *ABAQUS/Standard 6.1 User's Manual*, 1800 Main Street, Pantucket, RI 20860-4847.

[13] Litvin, F. L., 1968, *Theory of Gearing*, Nauka (in Russian), Moscow.

[14] Litvin, F. L., 1989, *Theory of Gearing*, NASA RP-1212 (AVSCOM 88-C-C035), Washington, D. C.

[15] Litvin, F. L., 1998, *Development of Gear Technology and Theory of Gearing*, NASA Reference Publication 1406, ARL-TR-1500.

[16] Press, W. H., Teukolsky, S. A., Vetterling, W. T., and Flannery, B. P., 1992, *Numerical Recipes in Fortran 77: The Art of Scientific Computing*, Cambridge University Press, New York, 2nd Ed.

[17] Zienkiewicz, O. C., and Taylor, R. L., 2000, *The Finite Element Method*, John Wiley & Sons, 5th Ed.